POWER EFFICIENCY OF TAPERED PROBE AND IT INFLUENCE ON RESOLUTION IN SCANNING NEAR-FIELD OPTICAL MICROSCOPY

Pavel TOMÁNEK, Pavel ŠKARVADA
Department of Physics, Faculty of Electrical Engineering and Communication,
Brno University of Technology, Technická 8, 616 00 Brno, Czech Republic, tel.: +420 541 143 278, e-mail: tomanek@feec.vutbr.cz

ABSTRACT

Novel optical techniques such as near-field come in a study of local properties of transparent or opaque microscopic structures such as optical waveguides, optoelectronic integrated circuits, photonic crystals, semiconductor interfaces, nanostructured systems. To control a light-matter interaction at nanometer distance, structures guiding electromagnetic energy with lateral mode confinement below the diffraction limit of light are necessary. Tapered optical fiber probe is a crucial part of the system, governs its resolution, and simultaneously could play role as light source and/or detector. The paper brings a simulation of losses, taking into account its correctly described geometry, as well as experimental verification of resolution obtained with this probe.

Keywords: *light-matter interaction, near field, optics, taper, radiation, loss, efficiency, resolution*

1. INTRODUCTION

The analysis of light propagation in tapered waveguides has been of great interest since the first inception of optoelectronic integrated circuits, and presently with the development of scanning near-field optical techniques [1,2]. Tapered optical fiber, which aperture is smaller than wavelength, is a crucial part of the system, governs its resolution, and plays role of tiny light source, detector, or both.

This lateral resolution of Scanning Near-field Optical microscopy (SNOM), which is one of its most important features, strongly depends on the dimensions and shape of the probe tip. To make optical fiber probes for SNOM, the chemical etching or pulling methods are usually applied to secure an appropriate smooth surface of the probe as well as its cone angle. The difference between them results in a shape of the tip [3]. In the first case, the core and cladding diameters decrease continuously, while in the second case, the diameter of the cladding is the same as in original fiber, and only fiber core decreases in its diameter.

To ensure that light comes only through the tip apex (optical aperture) and preserve the tip from the mechanical oscillations and damage, it is important to enhance its strength and cover it by dielectric or metallic thin film layer [4].

For accurate simulation of fiber shape, it is essential that its geometry is correctly described, especially when coupling to evanescent field is considered. One of the first approaches to be considered is to reduce the two dimensional waveguide cross section to one dimensional one, and thus analyse the simpler problem of propagation in a nominally equivalent 2D structure [5,6]. Such analyses subsequently provided a good insight into the loss mechanisms of fully three dimensional tapers. Excellent review of methods dealing with the analysis of waveguides is done in [7] and applied to the simulation of propagation in both 2D and 3D structures.

2. TAPERED PROBE

Consider the TE polarisation with $Ey = 0$. To solve the problem, we ponder here the modification of half-space radiation method (HSRM) method, that works [8] in the spectral domain, derived by means of a two dimensional Fourier transform (FT): an exponential FT is applied in the x – direction and a sine FT is applied in the y direction. Let p be the x-directed Fourier variable and s be y-directed one. The Fourier transformed components of the electric and magnetic fields, Ex and Hy, of the guided mode are denoted by $\tilde{e}^{\pm}(p,s)$ and $\tilde{h}^{\pm}(p,s)$. These modes can be obtained by HSRM method. For convenience, and for the reason that most of optical probes are made from single-mode fiber, only one mode is assumed in each guide, although the extension to multi-moded structures in telecommunications is straightforward [9].

Let us suppose, that in the core of original non-modified fiber waveguide 1, the known amplitudes of the guided mode and the radiation field incident on a step discontinuity are a^- and $\tilde{a}_r^-$ respectively, and amplitudes of the guided mode and the radiation field reflected from the discontinuity are b^- and $\tilde{b}_r^-$ respectively. Similarly, in the sector 2, first part of modified fiber, the amplitudes of the relevant fields are a^+, $\tilde{a}_r^+$, b^+ and $\tilde{b}_r^+$. Superscripts - and + denote the left and right side of the waveguide interface respectively, as shown in Fig. 1. It should be remembered that $\tilde{a}_r^{\pm}$ and $\tilde{b}_r^{\pm}$ depend upon s and p.

If we only consider the junction of two sectors of the tip, the guided modes in both are normalised such that

$$\int_{-\infty}^{\infty} dp \int_{0}^{\infty} ds \tilde{e}^{\pm}(p,s)(\tilde{h}^{\pm}(p,s))^{*} = 1 \tag{1}$$

At the junction, the continuity of the transverse electric and magnetic field components requires that

$$(a^- + b^-)\tilde{e}^- + \tilde{a}_r^- + \tilde{b}_r^- = (a^+ + b^+)\tilde{e}^+ + \tilde{a}_r^+ + \tilde{b}_r^+ \tag{2}$$

$$(a^- + b^-)\tilde{h}^- + Y_r^-(\tilde{a}_r^- - \tilde{b}_r^-) = (a+b)\tilde{e}^+ + \tilde{a}_r^+ + \tilde{b}_r^+ , \tag{3}$$

where $\tilde{Y}_r^-$ and $\tilde{Y}_r^+$ are the admittances of the sectors 1 and 2 respectively, i.e.,

$$Y_r^{\pm} = \frac{(k_{un}^{\pm})^2 - s^2}{\omega\mu\gamma^{\pm}}, \tag{4}$$

where

$$\gamma^{\pm} = \begin{cases} ((k_{un}^{\pm})^2 - p^2 - s^2)^{\frac{1}{2}}, (k_{un}^{\pm})^2 - p^2 - s^2 > 0 \\ -j((k_{un}^{\pm})^2 - p^2 - s^2), (k_{un}^{\pm})^2 - p^2 - s^2 < 0 \end{cases}, \tag{5}$$

with k_{un} the background wavenumber of the uniform medium in which the radiation field is assumed to propagate.

Eqs. (2) and (3) can be compactly represented in a matrix form as

$$\underline{\underline{F}}_a \underline{a} + \underline{\underline{F}}_b \underline{b} + \underline{\underline{Y}}_a \underline{a}_r + \underline{\underline{Y}}_b \underline{b}_r = 0, \tag{6}$$

where

$$\underline{\underline{F}}_a = \begin{bmatrix} \tilde{e}^- & -\tilde{e}^+ \\ \tilde{h}^- & \tilde{h}^+ \end{bmatrix}, \quad \underline{\underline{F}}_b = \begin{bmatrix} \tilde{e}^- & -\tilde{e}^+ \\ -\tilde{h}^- & -\tilde{h}^+ \end{bmatrix} \tag{7}$$

$$\underline{a} = \begin{bmatrix} a^- \\ a^+ \end{bmatrix}, \quad \underline{b} = \begin{bmatrix} b^- \\ b^+ \end{bmatrix} \tag{8}$$

$$\underline{\underline{Y}}_a = \begin{bmatrix} 1 & -1 \\ Y_r^- & Y_r^+ \end{bmatrix}, \quad \underline{\underline{Y}}_a = \begin{bmatrix} 1 & -1 \\ -Y_r^- & -Y_r^+ \end{bmatrix}, \tag{9}$$

$$\underline{a}_r = \begin{bmatrix} \tilde{a}_r^- \\ \tilde{a}_r^+ \end{bmatrix}, \quad \underline{b}_r = \begin{bmatrix} \tilde{b}_r^- \\ \tilde{b}_r^+ \end{bmatrix}. \tag{10}$$

From (6) the amplitudes of the reflected radiation field can be explicitly expressed in terms of the known guided mode profiles and incident amplitudes as

$$\underline{b}_r = -\underline{\underline{Y}}_b^{-1} (\underline{\underline{F}}_a \underline{a} + \underline{\underline{F}}_b \underline{b} + \underline{\underline{Y}}_a \underline{a}_r). \tag{11}$$

The guided mode is required to be orthogonal to the radiation field in each cylindrical sector, i.e.

$$\left\langle \underline{\underline{E}}, \underline{b}_r \right\rangle = 0, \tag{12}$$

where

$$\underline{\underline{E}} = \begin{bmatrix} e^- & 0 \\ 0 & e^+ \end{bmatrix}, \tag{13}$$

and the inner product denotes

$$\langle l, k \rangle = \int_{-\infty}^{\infty} dp \int_0^{\infty} ds (l^T).k. \tag{14}$$

Replacing (11) into (12) yields the reflected amplitudes of the guided mode

$$\underline{b} = -\left\langle \underline{\underline{E}}, \underline{\underline{Y}}_b^{-1} \underline{\underline{F}}_b \right\rangle^{-1} \left[\left\langle \underline{\underline{E}}, \underline{\underline{Y}}_b \underline{\underline{F}}_a \right\rangle \underline{a} + \left\langle \underline{\underline{E}}, \underline{\underline{Y}}_b^{-1} \underline{\underline{Y}}_a \underline{a}_r \right\rangle \right] \tag{15}$$

Now the amplitudes of the reflected guided and radiation fields are found from Eqs. (14) and (11) respectively, which completes the analysis.

The results for the power of the reflected guided mode, transmitted guided mode, the power of the radiation field and the power loss will be obtained using following formulae

$$P^- = \left| b^- \right|^2, \quad P^+ = \left| b^+ \right|^2, \tag{16}$$

$$P_r = \left| \int_{-\infty}^{\infty} dp \int_0^{\infty} ds \left[\tilde{b}_r^- (Y_r^- \tilde{b}_r^-)^* + \tilde{b}_r^+ (Y_r^+ \tilde{b}_r^+)^* \right] \right|^2 \tag{17}$$

$$P_{loss} = 1 - \left| b^+ \right|^2, \tag{18}$$

respectively.

3. METHOD

In the case of tapered waveguides, the continuous taper function is approximated as a sequence of step discontinuities (a staircase approximation).

The taper of length L is segmented into N cylindrical steps each of length $\Delta\ell$. Therefore a procedure described in this section will consider the first (N-1) steps of the taper.

At each step discontinuity, the analysis described above determines the scattered field from the incident fields. Subsequently, the field scattered from each step discontinuity, namely, the reflected guided mode and the radiation field on the right hand side of a step, become the incident fields for the adjacent steps. This procedure follows to the last discontinuity, and in the case where reflections are strong, a two-way iterative procedure follows which takes into account all reflections produced at previous iteration, and is performed until results converge. Before proceeding, it is assumed that, as with Free Space Radiation Method (FSRM) propagation algorithms although the orthogonality between the radiation field and the guided mode is imposed at the steps, it will not still be satisfied after propagating because the radiation field is not an exact solution of the wave equation, which leads to unacceptable errors [10]. To overcome this, once the reflected fields have been propagated to the adjacent junctions, a correction must be applied to reinforce the orthogonality at this new step. In order to derive a suitable correction scheme it is convenient to consider a fictitious waveguide junction where there is no change in the waveguide dimensions. In this case, it is obvious that analysis should yield,

$$b^- = a^+, \; b^+ = a^-, \tag{19}$$

given that

$$\tilde{e}^- = \tilde{e}^+, \; \tilde{h}^- = \tilde{h}^+. \tag{20}$$

which gives in a compact form

$$\underline{F}_a = -\underline{F}_b \begin{bmatrix} 0 & 1 \\ 1 & 0 \end{bmatrix} = -\underline{F}_b \underline{S}_o \tag{21}$$

However, replacing (21) in (15) actually predicts that the amplitudes of the reflected guided modes are

$$\underline{b} = \underline{\underline{S}}_o \underline{a} - \left\langle \underline{\underline{E}}, \underline{\underline{Y}}_b^{-1} \underline{\underline{F}}_b \right\rangle^{-1} \left\langle \underline{\underline{E}}, \underline{\underline{Y}}_b^{-1} \underline{\underline{Y}}_a \underline{a}_r \right\rangle = \underline{\underline{S}}_o \underline{a} - \underline{\delta} \tag{22}$$

where δ is the error arising from the approximation of the radiation field. For the special case $Y^- = Y^+$, the error can be expressed as

$$\underline{\delta} = \left\langle \underline{\underline{E}}, \underline{\underline{Y}}_b^{-1} \underline{\underline{F}}_b \right\rangle^{-1} \left\langle \underline{\underline{E}}, \underline{a}_r \right\rangle . \tag{23}$$

Replacing (23) into (11) we could see that the radiation fields are slightly reduced as

$$\underline{b}'_r = K \left| \underline{b}_r - \underline{\underline{Y}}_b^{-1} \underline{\underline{F}}_b \underline{\delta} \right| , \tag{24}$$

where K is a constant that ensures the power conservation of the radiation field [11]. This correction is equivalent to re-enforcing orthogonality between the radiation field and guided mode.

4. RESULTS

This section firstly shows numerical results of the power efficiency or loss for a taper tip in a close proximity to the air boundary.

Here we consider a set of cylindric cross-sections of waveguide, which diameter varied per saltum along the taper length. Two different types of taper are considered – the linear and the exponential taper. Here the HSRM method is applied to analyze propagation in a taper structure. Linear and the exponential tapers are considered with original diameter of single mode fiber core of $d_1 = 10$ μm, and final one (at the fiber tip apex) $d_N = 50$ nm, where subscripts 1 and N indicate the first and the last waveguide section in the staircase approximation of the taper. The refractive indices of the cladding and core are $n_{cl} = 1.45$ and $n_{co} = 1.5$ and the operating wavelength is $\lambda = 632{,}8$ nm. The background index for radiation modes is taken to be $k_{un} = n_{cl}k_0$. Both tapers are divided into N sections of uniform length $\Delta\ell = 0.10$ μm. The dimensions of the exponential taper are smoothly varied with length.

The radiation losses or power efficiency inside the core of linear and exponential taper, are analysed in the Fig. 1 where the results for the percentage of radiation losses along the taper are plotted. Both the linear and exponential taper are modelled using sections of length $\Delta\ell$. The case of deeply buried taper (dashed lines) and the taper buried at D = 0.1 μm (solid lines) are considered. The radiation losses include the reflected radiation fields at both sides of the discontinuity.

The tip is fabricated from single mode fiber, by selective etching in the 40% solution of fluoride acid (HF). In this case the apex angle is close to 90°, and height of the tip is of 4 μm (Fig. 2).

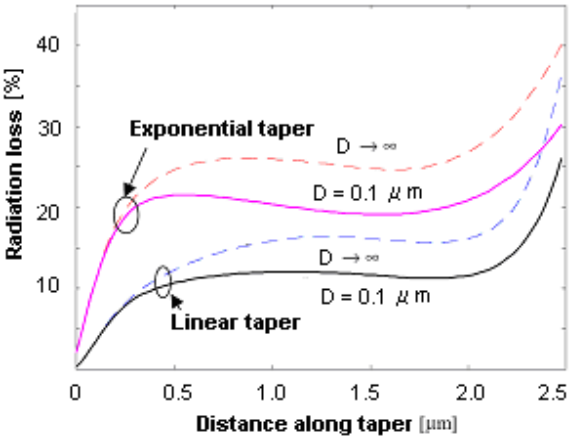

Fig. 1 Radiation losses vs distance along the taper for deeply buried tapers (dashed line) and taper buried at D = 0.1 μm (solid line). Both linear and exponential tapers are considered

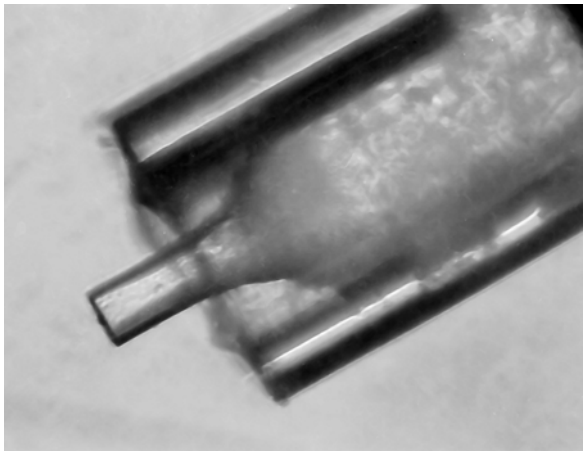

(a)

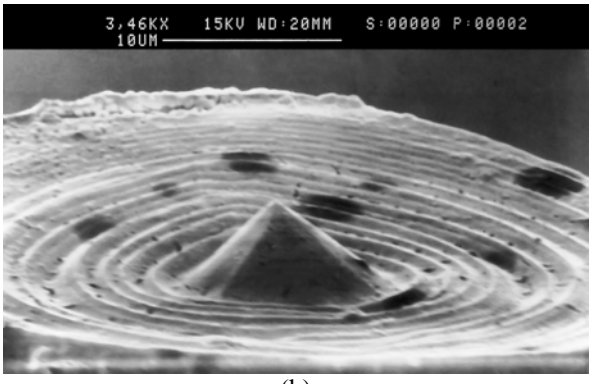

(b)

Fig. 2 a) Chemically etched optical fiber used for the signal detection in SNOM with plastic cladding protection against mechanical stress.
b) Detail of the fabricated tip on the end of the fiber core. In this linear shaped probe the efficiency of transmitted light is proportional to the tip cone apex [3].

Scanning Near-field optical microscopy SNOM is generally used for the investigation of quasi-planar objects, and in this case topographic artifacts occur rarely. On the other hand, if the surface is rough (in comparison with wavelength), and moreover contains abruptly

changed details, as in the case of monocrystalline silicon solar cells, the artifacts give a truncated image of the surface (Fig. 3).

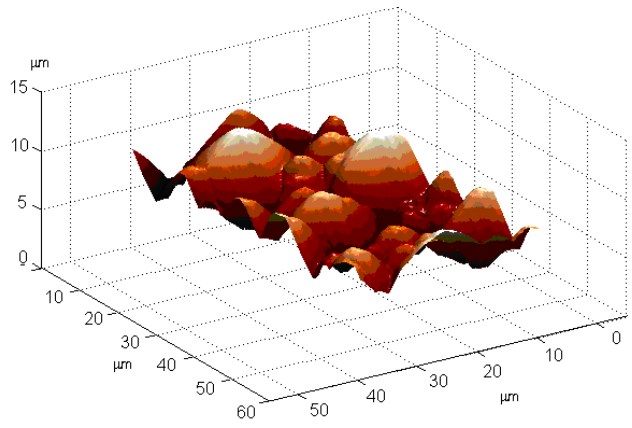

Fig. 3 Truncated topography of monocrystalline silicon solar cell due to the dimension of probe tip apex

To eliminate this inconvenient, and to increase the microscope resolution, the numerical calculation taking into account an ideal shape of the probe has been done. Fig. 4 shows the result of this lay-out. One can see that result is more realistic.

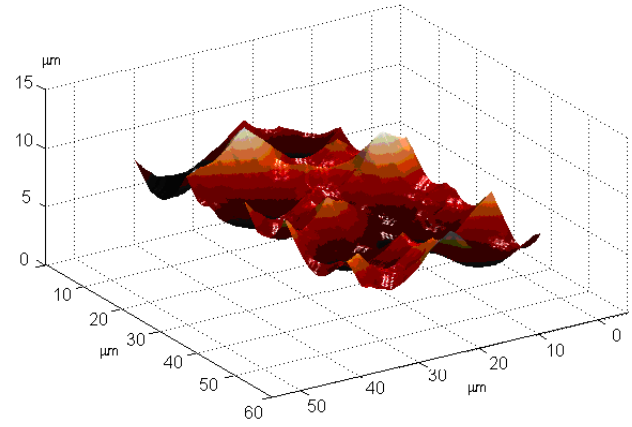

Fig. 4 Reconstruction of the image from Fig. 3 after elimination of the probe tip impact

5. CONCLUSIONS

The Half Space Radiation Mode method has been used to simulate field propagation along cylindric tapered waveguides. The waveguide geometry along its core is described using the staircase approximation.

It can be seen that shallowly buried taper exhibits smaller losses than deeply buried taper for both the linear and exponential taper. The linear taper again exhibits higher power efficiency than the exponential taper. It is noticeable that the radiation loss increases at the end of the taper which is due to increased radiation as the guided mode approaches the cut-off region defined by small dimensions of the guide. However, at the end of the taper, the total power loss and the power of the reflected radiation field are higher for the case of a shallowly buried waveguide.

The proposed experimental method allows to reduce artifacts originated from the peaks of the pyramids, and so to obtain a higher lateral resolution. In the case of quasiplanar surfaces, the scanning in two orthogonal directions is necessary. In the case of rough surfaces, the point of interest is punctual, therefore the scanning in one direction is quite sufficient for the reduction or removal of the artifacts from these rough surfaces.

On the other hand, the information about narrow deep valleys in the sample is in certain manner missing. The used probe tip generally scans an object by its apex, but also in some cases by the walls of its cone. Hence the method is only applicable to the rough surface having details smaller then apex diameter of the tip.

ACKNOWLEDGMENTS

This work has been supported by the Czech Ministry of Education in the frame of MSM 0021630503 Research Intention MIKROSYN "New Trends in Microelectronic System and Nanotechnologies" and by GAČR grant 102/08/1474 "Local optical and electric characterization of optoelectronic devices with nanometer resolution".

REFERENCES

[1] OTEVŘELOVÁ, D.: *Analysis of buried waveguides for mode spot converters*, In New trends in Physics, M. Štrunc, P. Dobis (Eds.), Ing. Zdeněk Novotný, Brno, pp. 254-257, 2004.

[2] MOERMAN, I. − VAN DAELE, P. P.− DEMEESTER, P. M.: A review on fabrication technologies for the monolithic integration of tapers with III-V semiconductor devices", *IEEE Journal of Selected Topics in Quantum Electronics*, Vol. 3, pp. 1308-1320, 1997.

[3] TOMANEK, P.: Fiber tips for reflection scanning near-field optical microscopy, In: D.W.Pohl, D. Courjon (Eds): *Near Field Optics*, Kluwer Academic Publishers, Dordrecht, pp. 295-302, 1993.

[4] ANTOSIEWICZ, T. J. – WRÓBEL, P. – SZOPLIK, T.: Nanofocusing of radially polarized light with dielectric-metal-dielectric probe, *Optics Express,* Vol. 17, No. 11, pp. 9191-9196, 2009

[5] SUCHOSKI, P. G. − RAMASWAMY, R.V.: Design of single mode step – tapered waveguide sections", *IEEE Journal of Quantum Electronics*, Vol. QE-23, pp. 206-211, 1987.

[6] TOMÁNEK, P. − BENEŠOVÁ, M. − DOBIS, P. − OTEVŘELOVÁ, D. − GRMELA, L. − KAWATA, S.: Near-field optical diagnostics of carrier dynamics in semiconductor with superresolution. *Physics of Low-dimensional structures*, No. 3/4, pp. 131-137, 2003.

[7] VUKOVIC, A. – SEWELL, P. − BENSON, T. M. − KENDALL, P. C.: Novel half space radiation mode

method for buried waveguide analysis, *Optical and Quantum Electronics*, Vol. 31, No. 1, pp. 43-51, 1999.

[8] OTEVŘELOVÁ, D. − TOMÁNEK, P.: Výpočet odrazivosti čela vlnovodu mělce vnořeného do polovodičového materiálu, *Jemná mechanika a optika*, Vol. 49, No. 9, pp. 245-247, 2004.

[9] KNOX, R. M. − TOULIOS, P. P.*: Integrated circuits for the millimeter through optical frequency range*, Proceedings of M.R.I. Symposium on Submillimeter waves, Fox J., Ed. Brooklyn, N. Y., Polytechnic Press, pp. 497- 503, 1970.

[10] BENSON, T. M. − SEWELL, P. − SUJECKI, S. − KENDALL, P. C.: Structure related beam propagation, *Optical and Quantum electronics*, Vol. 31, pp. 689-703, 1999.

[11] ŠKARVADA, P. – TOMÁNEK, P. – GRMELA, L.: *Influence of the SNOM probe shape on the object visualization*. In Nanooptics, Nanophotonics and Related Techniques*, NFO-10.* Universita Buenos Aires, pp. 189-190, 2008.

Received March 1, 2010, accepted July 7, 2010

BIOGRAPHIES

Pavel Tománek is a Professor in Applied Physics at Faculty of Electrical Engineering and Communication, Brno University of Technology since 2000. He is a chairman of EOS Scientific Advisory Committee (since 2002), Fellow EOS (2008), Member of SPIE, OSA, IEEE, Czech and Slovak Society for Photonics Execom (since 1992). Chairman of Photonics Prague conferences series, and SPIE Europe Congress on Optics and Optoelectronics. At present time, his main interest is Near-Field Optics and study of local optical and electronic properties of semiconductor and photonic devices.

Pavel Škarvada is a Ph.D. student in Physical Electronics and Nanotechnology at Faculty of Electrical Engineering and Communication, Brno University of Technology. His main interest is a study of optical and electronic properties of semiconductor and photonic devices, mainly solar cells.